Thermal properties of the nuclear surface

B. K. Agrawal, D. Bandyopadhyay, J. N. De, and S. K. Samaddar
Saha Institute of Nuclear Physics, 1/AF Bidhannagar, Kolkata 700064, India
(Received 12 November 2013; revised manuscript received 21 January 2014; published 22 April 2014)

The thermal evolution of a few thermodynamic properties of the nuclear surface like its thermodynamic potential energy, entropy, and the symmetry free energy are examined for both semi-infinite nuclear matter and finite nuclei. The Thomas-Fermi model is employed. Three Skyrme interactions, namely, SkM*, SLy4, and SK255, are used for the calculations to gauge the dependence of the nuclear surface properties on the energy density functionals. For finite nuclei, the surface observables are computed from a global liquid-drop-inspired fit of the energies and free energies of a host of nuclei covering the entire periodic table. The hot nuclear system is modeled in a subtracted Thomas-Fermi framework. Compared to semi-infinite nuclear matter, substantial changes in the surface symmetry energy of finite nuclei are indicated; surface thermodynamic potential energies for the two systems are, however, not too different. Analytic expressions to fit the temperature and asymmetry dependence of the surface thermodynamic potential of semi-infinite nuclear matter and the temperature dependence of the surface free energy of finite nuclei are given.

DOI: 10.1103/PhysRevC.89.044320 PACS number(s): 21.65.Cd, 21.65.Ef, 21.10.Dr

I. INTRODUCTION

The liquid-drop model provides a sound framework [1–3] for having a good estimate of the nuclear surface energy from experimental binding energy systematics. This is the case for cold nuclei; this has helped, for instance, in understanding barrier heights or saddle point configurations in nuclear fission. This estimate has also its place in the framing of effective nucleon-nucleon interactions [2,4] by providing an important empirical input. There is a strong motivation too to examine the thermal properties of the nuclear surface. Hot nuclei, produced in multifragmentation in nuclear collisions, are surrounded by nucleonic vapor; knowledge of the energy of the interface between the nuclear liquid and the vapor is a crucial determinant in their mass distributions [5,6] or in our understanding of their thermodynamic limit of existence [7,8]. This model has also important astrophysical applications. It puts significant constraints on determining the equilibrium nuclear masses, electron capture rates, and level densities that play a seminal role in the dynamical evolution of neutron stars and supernovae [9,10].

Semi-infinite nuclear matter (SINM) offers a good starting ground for exploring the nuclear surface properties. It has a simplicity coming from the absence of many undesirable complications arising from shell, Coulomb, and finite-size effects. Considerable effort has been directed in the past to understanding its surface properties at zero temperature, mostly in the semiclassical Thomas-Fermi (TF) framework [11–13]; studies have also been done using the quantal Hartree-Fock approach [14,15]. In a need for applications in an astrophysical scenario, Ravenhall, Pethick, and Lattimer in their pioneering work [16] explored the thermodynamic evolution of the surface properties of symmetric as well as asymmetric nuclear matter in the semiclassical approach using a plausible Skyrme interaction. With increasing temperature or asymmetry, the density of vapor consisting of hot or drip nucleons surrounding the liquid phase of the nuclear matter increases. The evolution of the interface energy with this change was quantitatively evaluated by them; they showed how the surface thermodynamic potential energy or the surface entropy eventually dissolves at a critical temperature when the distinction between the nuclear liquid and vapor is lost. A temperature dependence of the surface thermodynamic potential energy of the form $\{g[T,T_c(X)]\}^{\alpha_1}$ with $\alpha_1 = 1.25$ was suggested by them. The function $g[T,T_c(X)]$ has the form

$$g[T,T_c(X)] = \left\{\left[T_c^2(X) - T^2\right]\Big/\left[T_c^2(X) + T^2\right]\right\}, \qquad (1)$$

where $T_c(X)$ is the critical temperature for infinite nuclear matter of isospin asymmetry X, defined as $X = (\rho_n - \rho_p)/(\rho_n + \rho_p)$, where ρ_n and ρ_p are the neutron and proton densities (for SINM, the definition of asymmetry is somewhat more subtle and given later). Since then, numerous calculations have been done to understand properties of hot nuclear matter [5,6,17] with this form of temperature-dependent interface energy.

The scenario for finite nuclei is, however, different. The Coulomb interaction, coupled with the microscopic nuclear size, may influence the thermal evolution of their surface differently from that of the semi-infinite matter. It has already been noticed, in the course of the evaluation of the thermal dependence of volume and surface symmetry energy coefficients [18] of nuclei with a Skyrme-type KDE0 interaction and the finite-range modified Seyler-Blanchard interaction, that the surface thermodynamic potential of finite nuclear systems evolves in a slightly different way. The form of the evolution function $h(T) = g[T,T_c(X = 0)]$ is the same, but the exponent α_1 is seen to have a different value, slightly different for the two interactions. The hot nuclei undergo Coulomb instability at a limiting temperature [7], which is much lower compared to the critical temperature T_c. Consequently, the whole temperature range up to T_c is not accessible for the finite nuclei. The limiting temperature is generally a decreasing function of the atomic number [4,8].

On theoretical grounds, it is known that for infinite systems the surface thermodynamic energy behaves with temperature as $(T_c - T)^{\alpha_1}$, with $\alpha_1 = 1.26$ [19], but that is near the critical point. We note that for finite nuclei only a lower temperature

range can be mapped. In this case, the value of the calculated exponent is found different [18] from that found earlier in the case of SINM. We therefore intend to examine further in this article the evolution of the nuclear interface energy with temperature for semi-infinite nuclear matter, with a focus on the temperature range accessible to microscopic nuclei. Calculations are done in the TF approximation. To assess any possible dependence of the thermodynamic surface energy on effective nucleon-nucleon interaction, three Skyrme-class interactions, namely, SkM* [20], SLy4 [21], and SK255 [22], are employed in the calculations. These interactions obtained by accurately calibrating the bulk properties of finite nuclei over the whole periodic table are quite successful.

Because the setting for finite nuclear systems as stated earlier is somewhat different, calculations for their surface energies are also done with these interactions. Hot nuclei, because of evaporation are inherently unstable. To give stability, the subtraction procedure was first suggested by Bonche, Levit, and Vautherin [23,24] in the Hartree-Fock framework. In the present work, we adopt its semiclassical variant, the finite-temperature Thomas-Fermi (FTTF) scheme [25]. This ensures complete thermodynamic equilibrium between the high-density central liquid and the low-density surrounding nucleon gas. For a set of doubly closed shell and singly closed shell nuclei covering almost the entire periodic table, the energies and free energies are calculated in the FTTF scheme as a function of temperature. When subjected to analysis in the framework of the Bethe-Weizsäcker liquid-drop mass formula, they yield temperature-dependent surface thermodynamic entities.

The paper is organized as follows. Section II is devoted to the theoretical formulation of the study of the thermodynamic properties of the surface of asymmetric semi-infinite nuclear matter and of finite nuclei. Results and discussions are presented in Sec. III. Conclusions are drawn in Sec. IV.

II. THE NUCLEAR SURFACE PROPERTIES: THE MODEL

Determination of the equilibrium density distribution of the hot nuclear systems is the starting point for calculations of the thermodynamic properties of the nuclear surface. To describe a hot system as a stable one, it is assumed to be in thermal equilibrium with a surrounding gas representing the evaporated nucleons. Even a very asymmetric cold nuclear system may be stable beyond the nucleon drip point, the required stability being given by the drip nucleons [13,26]. The description of such a nuclear liquid embedded in a gaseous environment can be given in the FTTF framework. Section II A describes the procedure for obtaining the equilibrium density profiles for semi-infinite nuclear matter as well as for finite nuclei. Sections II B and II C give a brief glimpse of how the different surface properties are established from these density profiles.

A. Equilibrium density profiles

The method to obtain the equilibrium density profiles of semi-infinite matter and of finite systems is based on the existence of two solutions to the TF equations, one corresponding to the liquid phase with the surrounding gas (lg) and the other corresponding to the gas (g) alone. The two solutions are obtained from the variational equations

$$\frac{\delta\Omega_{\rm lg}}{\delta\rho_{\rm lg}} = 0 \tag{2}$$

and

$$\frac{\delta\Omega_{g}}{\delta\rho_{g}} = 0, \tag{3}$$

where $\Omega_{\rm lg}$ and Ω_g are the thermodynamic potentials of the said systems. These two systems have the same chemical potentials μ because of thermodynamic coexistence between the liquid plus gas system and the embedding gas (i.e., $\mu^q_{\rm lg} = \mu^q_g = \mu_q$, q refers to the isospin index for neutrons or protons). The base density profile of the nuclear liquid (l) of interest is obtained by subtracting the gas density (g) from that of the liquid plus gas system (lg), i.e., $\rho^q_l = \rho^q_{\rm lg} - \rho^q_g$. The thermodynamic potential is given by

$$\Omega = F - \sum_q \mu_q N_q, \tag{4}$$

where $F = E - TS$; F, E, and S are the total free energy, energy, and entropy, respectively; T is the temperature; N_q is the number of neutrons or protons; and μ_q is the corresponding chemical potential.

We have calculated the total energy with Skyrme interaction energy density functionals. The energy density is

$$\mathcal{E}(r) = \frac{\hbar^2}{2m_n}\tau_n(r) + \frac{\hbar^2}{2m_p}\tau_p(r) + \mathcal{E}_{\rm sky}[\rho(r)] + \mathcal{E}_c(r), \tag{5}$$

where τ's are the kinetic energy densities, $\mathcal{E}_{\rm sky}$ is the interaction energy density, and $\mathcal{E}_c$ is the Coulomb energy density. The Skyrme interaction energy density is given by

$$\begin{aligned}\mathcal{E}_{\rm sky}[\rho(r)] = {}& \frac{1}{2}t_0\left[\left(1+\frac{1}{2}x_0\right)\rho^2 - \left(x_0+\frac{1}{2}\right)\left(\rho_n^2+\rho_p^2\right)\right] + \frac{1}{12}t_3\rho^\gamma\left[\left(1+\frac{x_3}{2}\right)\rho^2 - \left(x_3+\frac{1}{2}\right)\left(\rho_n^2+\rho_p^2\right)\right] \\ & + \frac{1}{4}\left[t_1\left(1+\frac{1}{2}x_1\right) + t_2\left(1+\frac{1}{2}x_2\right)\right]\tau\rho + \frac{1}{4}\left[t_2\left(x_2+\frac{1}{2}\right) - t_1\left(x_1+\frac{1}{2}\right)\right](\tau_n\rho_n + \tau_p\rho_p) \\ & + \frac{1}{16}\left[3t_1\left(1+\frac{1}{2}x_1\right) - t_2\left(1+\frac{1}{2}x_2\right)\right](\nabla\rho)^2 - \frac{1}{16}\left[3t_1\left(x_1+\frac{1}{2}\right) + t_2\left(x_2+\frac{1}{2}\right)\right][(\nabla\rho_n)^2 + (\nabla\rho_p)^2],\end{aligned} \tag{6}$$

TABLE I. The values of the Skyrme parameters for SkM*, SLy4, and SK255 interactions.

Parameters	SkM*	SLy4	SK255
t_0(MeV fm^3)	−2645.0	−2488.91	−1689.35
t_1(MeV fm^5)	410.0	486.82	389.30
t_2(MeV fm^5)	−135.0	−546.39	−126.07
t_3(MeV fm$^{3(\gamma+1)}$)	15 595.0	13 777.0	10 989.59
x_0	0.09	0.834	−0.1461
x_1	0.0	−0.344	0.116
x_2	0.0	−1.0	0.0012
x_3	0.0	1.354	−0.7449
γ	0.1666	0.1666	0.3563

with $\tau = \tau_n + \tau_p$ and $\rho = \rho_n + \rho_p$. Here the t_i's, x_i's, and γ are the Skyrme parameters listed in Table I, for the three chosen interactions. The Coulomb contribution is present in Eq. (5) only for finite nuclei; they cannot be treated for both homogeneous nuclear matter and semi-infinite nuclear matter.

In Eq. (6), we have not included the spin-gradient terms [27] because they were ignored while fitting the parameters for the Skyrme forces we have chosen.

At finite temperature, the effective kinetic energy density is [27]

$$\tau_q^* = \frac{2m_q^*}{\hbar^2} A_{T,q}^* T J_{3/2}(\eta_q), \tag{7}$$

with

$$A_{T,q}^* = \frac{1}{2\pi^2}\left(\frac{2m_q^* T}{\hbar^2}\right)^{3/2}. \tag{8}$$

In Eqs. (7) and (8), m_q^* is the nucleon effective mass,

$$m_q^* = m\left(1 + \frac{m}{2\hbar^2}\left\{\left[t_1\left(1+\frac{x_1}{2}\right) + t_2\left(1+\frac{x_2}{2}\right)\right]\rho + \left[t_2\left(x_2+\frac{1}{2}\right) - t_1\left(x_1+\frac{1}{2}\right)\right]\rho_q\right\}\right)^{-1}, \tag{9}$$

and η_q the fugacity,

$$\eta_q = (\mu_q - U_q)/T. \tag{10}$$

In Eq. (10), U_q is the nucleon single-particle potential,

$$U_q = \frac{\delta\{\mathcal{E}_{\rm sky}[\rho(r)] + \mathcal{E}_c\}}{\delta\rho_q}, \tag{11}$$

with the symbol δ referring to the functional derivative here. For neutrons, $\mathcal{E}_c = 0$. The density ρ_q is obtained as

$$\rho_q = A_{T,q}^* J_{1/2}(\eta_q). \tag{12}$$

The J_k's are the Fermi integrals. The $T = 0$ case is a special case which can be addressed easily from Eqs. (7)–(12). The Coulomb energy density $\mathcal{E}_c(r)$ is the sum of the direct and exchange contributions:

$$\mathcal{E}_c(r) = \mathcal{E}_c^D(r) + \mathcal{E}_c^{\rm Ex}(r). \tag{13}$$

The direct term is

$$\mathcal{E}_c^D(r) = \pi e^2 \frac{\rho_p(r)}{r}\int_0^\infty \rho_p(r')[(r+r') - |r-r'|]r'dr', \tag{14}$$

and the exchange term is calculated from the Slater approximation as

$$\mathcal{E}_c^{\rm Ex}(r) = \frac{-3e^2}{4\pi}(3\pi^2)^{1/3}\rho_p^{4/3}(r). \tag{15}$$

The entropy density $\mathcal{S}$ is the sum of contributions from neutrons and protons:

$$\mathcal{S} = \sum_q \mathcal{S}_q = \sum_q \left(\frac{5}{3}\frac{\hbar^2}{2m_q^*}\frac{\tau_q^*}{T} - \eta_q\rho_q\right). \tag{16}$$

From Eqs. (2) and (3), the coupled equations follow:

$$T\eta_{\rm lg}^q + U_{\rm lg}^q = \mu_q, \tag{17}$$

$$T\eta_g^q + U_g^q = \mu_q. \tag{18}$$

Solutions of the above two equations yield the required density profiles $\rho_{\rm lg}^q(r)$ and $\rho_g^q(r)$. The calculations proceed as follows: from guess densities $\rho_{\rm lg}^q(r)$ and $\rho_g^q(r)$, one calculates U_q and η_q from Eqs. (9)–(12) and then obtains μ_q as

$$\mu_q = \frac{1}{A_q}\left\{\int\left[T\eta_{\rm lg}^q + U_{\rm lg}^q\right]\rho_{lg}^q d^3r - \int\left[T\eta_g^q + U_g^q\right]\rho_g^q d^3r\right\}, \tag{19}$$

where A_q is the neutron or proton number of the subtracted liquid part,

$$A_q = \int\left[\rho_{\rm lg}^q(r) - \rho_g^q(r)\right]d^3r. \tag{20}$$

With this μ_q, one can calculate η_q with the previous U_q, obtaining the next stage densities ρ_q through Eq. (12), and proceed iteratively until convergence is achieved.

For a finite system, A_q refers to the actual number of neutrons (N) or protons (Z) in the nucleus one is dealing with. For semi-infinite system, one chooses for calculation a sufficiently large box size and suitable number of nucleons so that both ρ_g and $\rho_{\rm lg}$ attain constant values at large and short distances, respectively (the two extreme ends of the box as shown in Fig. 1). The asymptotic constancy of $\rho_{\rm lg}$ and ρ_g at $z \to -\infty$ and $z \to +\infty$, respectively, is assured this way.

B. Calculation of surface energy coefficients: Semi-infinite matter

In the context of the subtraction method for the isospin asymmetric semi-infinite nuclear system, there could be two definitions [11,13] of the nuclear interface energy. The definitions differ depending on whether one calculates the change in the total free energy or that in the total thermodynamic potential of the semi-infinite matter from the corresponding quantities of the bulk matter. The subtraction of the constant gas density from that of the liquid plus gas does not change the surface profile of the semi-infinite matter (see Fig. 1). Delineating the liquid density (l) one can define the surface

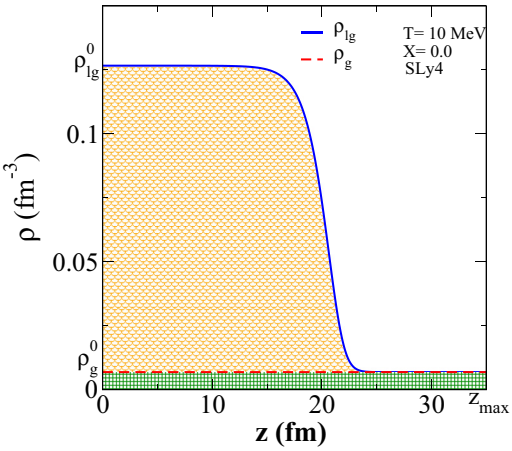

FIG. 1. (Color online) The density profiles for liquid plus gas ($\rho_{\rm lg}$) and gas (ρ_g) for symmetric semi-infinite nuclear matter at $T = 10$ MeV with the SLy4 interaction. The green-shaded region and the orange-shaded region represent the gas and the liquid density distributions, respectively.

free energy per unit area σ_e [11,13] from

$$F_A = Af_B^l + \sigma_e \mathcal{A}, \tag{21}$$

where F_A is the total free energy of the semi-infinite liquid (l) containing A nucleons in a cylinder of area of cross section $\mathcal{A}$ normal to the liquid surface and f_B^l is the free energy per particle of the homogeneous bulk liquid. It may be pointed out that the actual calculations are performed over a finite range of z, $o \leqslant z \leqslant z_{\rm max}$ (see Fig. 1), so that the total number of nucleons A in the said cylinder in the liquid is finite.

From Eq. (21), one gets the following for σ_e,

$$\sigma_e = \int_0^{z_{\rm max}} dz[\mathcal{F}_{\rm lg}(z) - \mathcal{F}_g(z)] - Af_B^l/\mathcal{A}. \tag{22}$$

Using the expression for f_B^l, one finds

$$\sigma_e = \int_0^{z_{\rm max}} dz\left\{[\mathcal{F}_{\rm lg}(z) - \mathcal{F}_g(z)] - [\rho_{\rm lg}(z) - \rho_g(z)]\frac{\mathcal{F}_{\rm lg}^0 - \mathcal{F}_g^0}{\rho_{\rm lg}^0 - \rho_g^0}\right\}, \tag{23}$$

where we have used Eq. (20) for the evaluation of A.

In Eq. (23), $\mathcal{F}_{\rm lg}$, $\mathcal{F}_g$, etc. are the free energy densities, the superscript 0 referring to the corresponding bulk quantities. It may be noted that $\mathcal{F}_g(z) = \mathcal{F}_g^0$ because the gas density is constant throughout.

The surface thermodynamic potential per unit area σ_μ can likewise be defined from

$$\Omega_A = \Omega_B^l + \sigma_\mu \mathcal{A}, \tag{24}$$

whence

$$\sigma_\mu = \int_0^{z_{\rm max}} dz\big\{\mathcal{F}_{lg}(z) - \mathcal{F}_g^0 - \mu_n\big[\rho_{\rm lg}^n(z) - \rho_g^n\big] - \mu_p\big[\rho_{\rm lg}^p(z) - \rho_g^p\big]\big\}. \tag{25}$$

In Eq. (24), $\Omega_B^l = -(P_{lg}^0 - P_g^0)\mathcal{A}z_{\rm max}$, where P^0 refers to the bulk pressure. For thermodynamic equilibrium, the pressure $P_{\rm lg}^0 = P_g^0$; hence the bulk thermodynamic potential of the liquid (l) $\Omega_B^l = 0$. Further, $\mu_{\rm lg}^n = \mu_g^n = \mu_n$ and $\mu_{\rm lg}^p = \mu_g^p = \mu_p$.

For isospin asymmetric systems, these two definitions given by Eqs. (23) and (25) yield different surface interface energies. The difference is given by [13]

$$\sigma_e - \sigma_\mu = (\mu_n - \mu_p)(R_n - R_p)\frac{\rho_{ln}^0 \rho_{lp}^0}{\rho^0}, \tag{26}$$

where R_n and R_p are the equivalent sharp surface locations (in the spirit of the liquid-drop model) of the neutron and proton fluid; $\rho_{\rm ln}^0, \rho_{\rm lp}^0$ are the bulk neutron and proton densities in the liquid and $\rho^0 = \rho_{\rm ln}^0 + \rho_{\rm lp}^0$. For symmetric matter, the two definitions yield identical results.

C. Calculation of surface energy coefficients: Finite nuclei

Unlike SINM, isospin asymmetry does not fully define the surface characteristics of atomic nuclei. With the same isospin asymmetry, there may be nuclei with different neutron and proton numbers; the surface properties of nuclei may thus be somewhat different. In that sense, one can talk meaningfully only about average surface properties of nuclei. To calculate the surface interface energy of hot finite systems, we limit ourselves to the liquid-drop framework. In that model, the total free energy of a nucleus is given by

$$F(A,Z,T) = f_v(T)A + f_s(T)A^{2/3} + E_c(A,Z,T) + \big(f_v^{\rm sym}(T) - f_s^{\rm sym}(T)A^{-1/3}\big)AX^2 + \ldots, \tag{27}$$

where f_v and f_s are the volume and the surface free energy coefficients for the symmetric matter, E_c is the total Coulomb energy of the nucleus, and $f_v^{\rm sym}$ and $f_s^{\rm sym}$ are the volume and surface free symmetry energy coefficients. Here $X = (N - Z)/A$ is the isospin asymmetry of the nucleus. Referring to our discussion in the previous subsection, one wonders whether $(f_s - f_s^{\rm sym}X^2)$ should be connected with σ_e or σ_μ. It has been argued in Ref. [11] that in the context of the liquid-drop model, it should be connected with σ_μ, the surface thermodynamic potential. We follow the prescription. To calculate the thermal dependence of this surface interface energy of finite nuclear systems, we evaluate, in the subtraction scheme, the free energies of a host of spherical or near-spherical nuclei, 69 in number (the list of nuclei is taken from Ref. [28]), covering almost the entire periodic table ($34 \leqslant A \leqslant 218; 14 \leqslant Z \leqslant 92$) at a finite temperature and make a least-squares fit of the calculated free energies with f_v, f_s, etc. as free parameters. In actual calculations, we fitted $F(A,Z,T) - E_c(A,Z,T)$, i.e., the nuclear part of the free energy. The four parameters, namely, $f_v, f_s, f_v^{\rm sym}$, and $f_s^{\rm sym}$, so fitted, reflect their desired temperature dependence.

III. RESULTS AND DISCUSSIONS

The calculations for SINM and for finite nuclei are done with three Skyrme interactions, SkM*, SLy4, and SK255. The actual calculations for SINM are done in a reasonably large box size. In Fig. 1, we display a typical density profile for symmetric SINM at the temperature $T = 10$ MeV with the

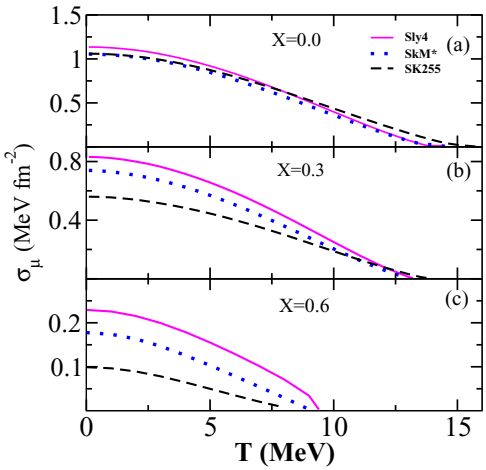

FIG. 2. (Color online) Thermal evolution of the surface thermodynamic potential σ_μ of SINM with the SLy4, SkM*, and SK255 interactions. Panels (a)–(c) display results for $X = 0.0$, 0.3, and 0.6, respectively.

SLy4 interaction. As seen in the figure, with a box size of 35 fm, the gas density on the right side of the box and the liquid plus gas density on the left side attain constant asymptotic values. The liquid density ρ_l shown by the orange-shaded region is obtained after subtracting the constant gas density ρ_g (shown by the green-shaded region) from the liquid plus gas density $\rho_{\rm lg}$. The quantities $\rho^0_{\rm lg}$ and ρ^0_g represent the bulk values for the liquid plus gas and gas densities, respectively. As seen in the figure, the choice of 35 fm for the maximum value of z ($z_{\rm max}$) suffices, provided a suitable value for the number of nucleons per unit area is chosen (in the present calculation, it is 2.5 per fm^2). For asymmetric SINM, the neutron and proton fractions in the liquid part and those in the gas part may be different. For the system in phase equilibrium, definition of global asymmetry of the whole system is then not practical; it depends on the size of the box. For numerical convenience, as in Refs. [13,16], we therefore define asymmetry as that of the denser side of SINM, i.e., $X = (\rho^0_{{\rm lg},n} - \rho^0_{{\rm lg},p})/(\rho^0_{{\rm lg},n} + \rho^0_{{\rm lg},p})$.

The thermal evolution of the surface thermodynamic potential per unit area σ_μ of SINM is shown in Fig. 2 for the three chosen interactions. Figures 2(a)–2(c) display calculated results for different asymmetries. The general feature seen is that σ_μ monotonically decreases with temperature, reaching zero at the critical temperature. The value of the critical temperature depends on the choice of interactions and asymmetries. That σ_μ depends on the choice of interactions is evident. This dependence is quite weak for symmetric matter, becoming pronounced with increasing asymmetry.

As shown in Ref. [19], near critical temperature, the surface thermodynamic potential $\sigma_\mu(T,X)$ goes as $(T_c(X) - T)^{\alpha_1}$ with $\alpha_1 \simeq 1.26$. Keeping this in mind, the commonly used temperature dependence of $\sigma_\mu(T,X)$ for SINM over the whole temperature range for all asymmetries is taken as [16]

$$\sigma_\mu(T,X) = \sigma_\mu(0,X)\{g[T,T_c(X)]\}^{\alpha_1}, \qquad (28)$$

TABLE II. The values of the parameters determining the surface interface energy as a function of temperature and asymmetry for the SkM*, SLy4, and SK255 interactions.

Parameters	SkM*	SLy4	SK255
$\sigma_\mu(0,0)$ (MeV fm^{-2})	1.055	1.135	1.060
C_0	6.445	12.079	−4.558
α_1	0.916	0.898	0.914
β	−0.184	−0.576	−0.344

where $g[T,T_c(X)]$ is given by Eq. (1) and $\alpha_1 = 5/4$. The asymmetry dependence of $\sigma_\mu(0,X)$ is taken as

$$\sigma_\mu(0,X) = \sigma_\mu(0,0)(16 + C_0)/[y^{-3} + C_0 + (1-y)^{-3}], \qquad (29)$$

where $y = (1-X)/2$ and C_0 a parameter. The plausibility of the dependence of $\sigma_\mu(0,X)$ on y^3 has its origin in the phase equilibrium conditions [16]. The critical temperature is asymmetry dependent.

From our calculation, we find that an algebraic expression of $\sigma_\mu(T,X)$ of the form

$$\sigma_\mu(T,X) = \sigma_\mu(0,0)\{g[T,T_c(X)]\}^{\alpha_1} \times \frac{16 + C_0\{g[T,T_c(X)]\}^\beta}{y^{-3} + C_0\{g[T,T_c(X)]\}^\beta + (1-y)^{-3}} \qquad (30)$$

gives an extremely good fit to the calculated values for $X \leqslant 0.7$ and $T \leqslant T_c(X = 0.7) \simeq 7.5$ MeV. Up to a value of $X = 0.7$, the asymmetry dependence of T_c can be well described by a polynomial of the form $T_c(X) = T_c(X = 0)[1 + aX^2 + bX^4]$. The values of a are −0.9238, −0.8126, and −1.2654, the values of b are −0.3529, −0.4193, and 0.1158 for SkM*, SLy4, and SK255 interactions, respectively. The values of $\sigma_\mu(0,0)$, α_1, C_0, and β are given in Table II for the three chosen interactions. The value of α_1 is seen to be ∼0.9 in this temperature range. It has been checked that this value gradually rises to the canonical value of ≃1.26 in a narrow temperature

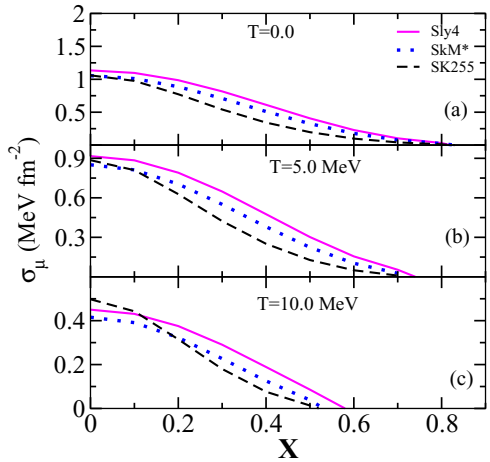

FIG. 3. (Color online) The surface thermodynamic potential σ_μ of SINM with the three interactions plotted as a function of isospin asymmetry. Panels (a)–(c) show results at temperatures $T = 0.0$, 5.0, and 10.0 MeV, respectively.

window near the critical temperature. The critical temperatures $T_c(X=0)$ are 14.61, 14.53, and 15.98 MeV for SkM*, SLy4, and SK255 interactions, respectively. In Fig. 3, the asymmetry dependence of σ_μ is displayed for the same interactions at three temperatures, namely, at $T=0$, 5, and 10 MeV in the panels (a)–(c), respectively. The surface potential $\sigma_\mu(T,X)$ decreases with both temperature and asymmetry, reaching zero at $T_c(X)$. One can see that the temperature- and asymmetry-dependent $\sigma_\mu(T,X)$ has a non-negligible dependence on the interactions one chooses to describe the SINM with.

The external gas surrounding nuclear drops in clusterized nuclear matter in an astrophysical environment has its origin in both temperature and asymmetry. Even at $T=0$, nuclei may exist embedded in a nucleon gas in an astrophysical environment [26,29] leading to the modification of the nuclear properties. In Ref. [29], Papakonstantinou *et al.* find an increase in surface energy with an increase in asymmetry for cold nuclei in contradiction to what we find for SINM from Eq. (30) with $T=0$. It may possibly be attributed to different definitions of the surface energy (σ_e is known to increase initially with asymmetry [13]). Part of the reason may also lie in the definition of the asymmetry parameter; X in our case is the asymmetry of the denser part of the liquid-gas system, while in Ref. [29] the asymmetry defined is that of the subtracted liquid part.

The temperature dependence of the surface symmetry energy coefficient $f_s^{\rm sym}$ for SINM is shown in Fig. 4. In keeping with the convention used for finite systems [as is employed in Eq. (27)], we define $f_s^{\rm sym}$ as

$$f_s^{\rm sym}(T)=\left[-4\pi r_0^2(T)\frac{1}{2}\frac{d^2\sigma_\mu(T,X)}{dX^2}\right]_{X=0}, \qquad (31)$$

where the radius parameter $r_0(T)=1/[\frac{4}{3}\pi\rho_l^0(T)]^{1/3}$, $\rho_l^0(T)$ being the bulk liquid density of symmetric matter at the temperature concerned. From Eqs. (30) and (31), one then gets

$$f_s^{\rm sym}(T)=4\pi r_0^2(T)\sigma_\mu(0,0)g^{\alpha-1}[T,T_c(X=0)] \times\left[\frac{96g[T,T_c(X=0)]}{16+C_0g^\beta[T,T_c(X=0)]}-\frac{4a\alpha T^2T_c^2(X=0)}{\left[T_c^2(X=0)+T^2\right]^2}\right]. \qquad (32)$$

For all the interactions, the surface symmetry energy decreases with temperature. It is evident from the figure that the calculated value of $f_s^{\rm sym}(T=0)$ for the SK255 interaction is around twice the value obtained from the other two interactions. The comparatively faster fall of σ_μ with asymmetry as seen in Fig. 2 for the SK255 interaction is a reflection of the larger value for the surface symmetry coefficient for this interaction. The properties of symmetric and asymmetric nuclear matter at the saturation density are quite different for the SK255 force compared to the other two interactions used. For example, the nuclear incompressibility coefficient, the volume symmetry energy coefficient, and the density slope parameter L ($=3\rho\frac{\partial f_v^{\rm sym}}{\partial\rho}$ at the saturation density of symmetric nuclear matter at $T=0$) are larger in comparison to those of the SkM* and SLy4 forces. The large value of $f_s^{\rm sym}(T=0)$ for SINM with the SK255 interaction can be qualitatively understood as being directly related to the corresponding large value of L ($\simeq$95 MeV for SK255 as compared to $\simeq$45 MeV for SLy4 or SkM*). For a heavy nucleus of mass number A, $f_s^{\rm sym}(T=0)$ is $\sim A^{1/3}[L\epsilon_A-\frac{K_{\rm sym}}{2}\epsilon_A^2]$ [30], where $K_{\rm sym}$ is the symmetry incompressibility and $\epsilon_A=(\rho_l^0-\rho_A)/(3\rho_l^0)$, ρ_A being the equivalent density for the nucleus. The quantity $\rho_l^0-\rho_A$ can be parametrized as $\rho_l^0-\rho_A\simeq\rho_l^0/(1+cA^{1/3})$ [31] (c is around 0.28 for terrestrial nuclei) so that, for a hypothetical chargeless large nuclear drop of mass A, ϵ_A is $\sim A^{-1/3}/(3c)$. For SINM, $f_s^{\rm sym}(T=0)$ is then $\sim L/(3c)$.

Entropy per unit area of the surface of semi-infinite matter is discussed in association with the following two figures. The

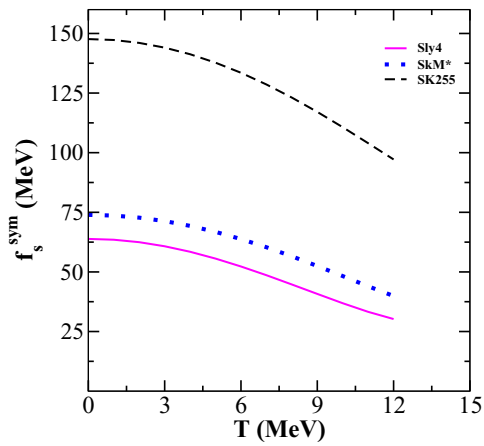

FIG. 4. (Color online) Thermal evolution of the surface symmetry free energy coefficient $f_s^{\rm sym}$ of SINM for the interactions SLy4, SkM*, and SK255.

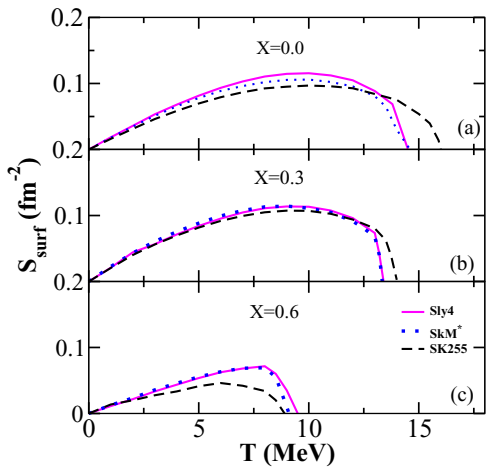

FIG. 5. (Color online) The surface entropy per unit area of SINM shown as a function of temperature for the three interactions at asymmetries $X=0.0$, 0.3, and 0.6.

surface entropy per unit area is defined as [16]

$$s_{\rm surf} = -\left.\frac{\partial\sigma_\mu(T,X)}{\partial T}\right|_{\mu_n} = -\left.\frac{\partial\sigma_\mu(T,X)}{\partial T}\right|_{X} + \left.\frac{\partial\sigma_\mu}{\partial X}\right|_{T} \frac{\left.\frac{\partial\mu_n}{\partial T}\right|_{X}}{\left.\frac{\partial\mu_n}{\partial X}\right|_{T}}. \quad (33)$$

In Fig. 5, the temperature dependence of $s_{\rm surf}$ is shown for three asymmetries ($X = 0.0$, 0.3, and 0.6). The thermal evolution of $s_{\rm surf}$ for all three interactions shows nearly the same behavior for all asymmetries; temperature raises the surface entropy as is expected, but after a maximum is reached, the entropy falls sharply as the interface and the energy associated with it dissolve near the critical point. In Fig. 6, the asymmetry dependence of the surface entropy is displayed at two temperatures, $T = 4.0$ and 8.0 MeV. No appreciable sensitivity either to the interaction or to X except at large values of asymmetry is noticed.

As discussed in Sec. II C, we have calculated the total free energies of the nuclei as a function of temperature in the subtracted FTTF procedure and then found the values of the parameters $f_v(T)$, $f_s(T)$, $f_v^{\rm sym}(T)$, and $f_s^{\rm sym}(T)$ from a least-squares fit. To be in concordance with the liquid-drop model of finite nuclei, a connection of $f_s(T)$ with $\sigma_\mu(T)$ [$\equiv \sigma_\mu(T, X = 0)$] for symmetric SINM is looked for, which can be established as

$$f_s(T) = 4\pi r_0^2(T)\sigma_\mu(T). \quad (34)$$

For finite nuclei, $r_0(T)$ can be defined from $r_0(T) = R_0(T)/A^{1/3}$, where $R_0(T)$ is its sharp surface radius. For semi-infinite matter, $r_0(T)$ is already defined in connection with Eq. (31). One can see that $f_s(T = 0) \sim 18$ MeV, with $r_0(T = 0) \sim 1.2$ fm [32].

The radius parameter $r_0(T)$ for both finite nuclei and symmetric SINM is seen to be fitted extremely well in the temperature range $T = 0$ to $T_{\rm lim}(\sim 7.5)$ MeV as defined for finite nuclei with the function $h(T) = g[T, T_c(X = 0)]$ as

$$r_0(T) = r_0(0)[h(T)]^{\alpha_2}, \quad (35)$$

TABLE III. Values of exponents α_1 and α_2 for symmetric SINM and for finite nuclei in the temperature range $T = 0$ to 7.5 ($\sim T_{\rm lim}$) MeV.

Interaction	Symmetric SINM			Finite nuclei		
	α_1	α_2	α	α_1	α_2	α
SkM*	0.966	−0.076	0.814	1.486	−0.222	1.042
SLy4	0.919	−0.069	0.781	1.404	−0.226	0.952
Sk255	1.019	−0.077	0.855	1.427	−0.208	1.011

so that $f_s(T)$ can be defined as

$$f_s(T) = 4\pi r_0^2(0)\sigma_\mu(0)[h(T)]^\alpha, \quad (36)$$

where $\alpha = \alpha_1 + 2\alpha_2$. The values for α_1, α_2, and α are listed in Table III for symmetric SINM as well as for finite nuclei for the three energy density functionals. From the table, one sees that the exponent α_1 governing the temperature dependence of the interface energy per unit area $\sigma_\mu(T)$ is significantly large for finite systems as compared to that for SINM. One further sees that the radius parameter $r_0(T)$ increases faster for finite systems. Overall, one finds that $f_s(T)$ values for symmetric SINM and for finite nuclei are not qualitatively very different though $f_s(T)$ seems to fall somewhat faster for finite nuclei. In Fig. 7, this general thermal behavior of $f_s(T)$ is displayed. The values of α_1, α_2, and α are seen to be nearly independent of energy density functionals. One may note that there are some differences in the values of α_1 for SINM in Tables II and III. This is because α_1 for SINM in Table III pertains to a small subset of data used for fitting (symmetric SINM). The thermal evolution of the surface symmetry free energy coefficient $f_s^{\rm sym}$ for finite nuclei is displayed for the three interactions in Figs. 8(a)–8(c) and compared with that of SINM. Comparatively the sensitivity of $f_s^{\rm sym}$ to temperature for finite nuclei is seen to be weaker. Strikingly, $f_s^{\rm sym}$ for semi-infinite matter is found to be much larger for all three interactions. This appears to be a finite-size

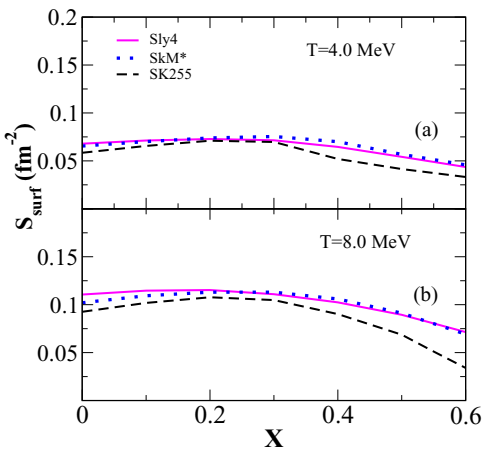

FIG. 6. (Color online) The surface entropy per unit area of SINM shown as a function of asymmetry for the three interactions at $T = 4.0$ and 8.0 MeV.

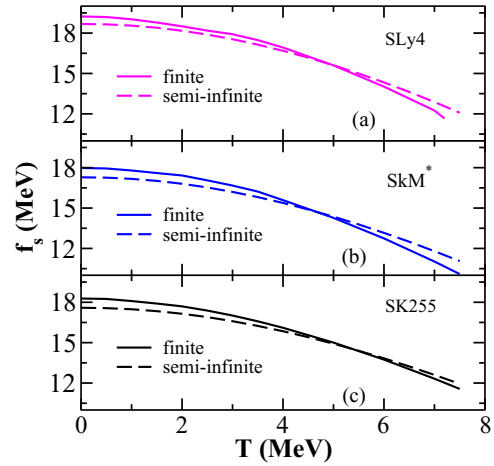

FIG. 7. (Color online) Comparison of the thermal evolution of the surface free energy f_s for finite nuclei (solid lines) and symmetric SINM (dashed lines) with the interactions SLy4, SkM*, and SK255.

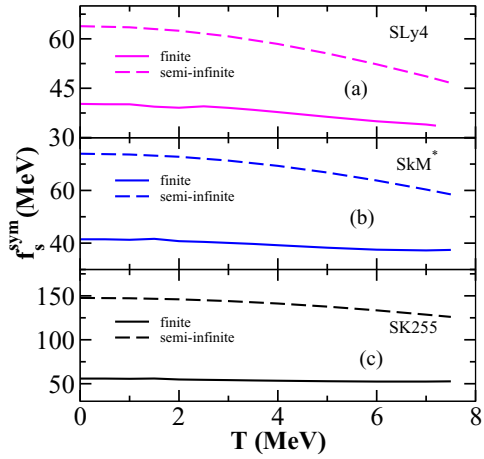

FIG. 8. (Color online) Comparison of the thermal evolution of the surface symmetry free energy coefficients for finite nuclei (solid lines) and symmetric SINM (dashed lines) for the three interactions.

effect. The Coulomb effect on $f_s^{\rm sym}$ is found to be nominal. Switching off the Coulomb interaction, we have tested that, as the nuclear size increases, $f_s^{\rm sym}$ approaches the asymptotic value for semi-infinite matter. We take a set of nuclei at a fixed temperature (say $A \sim 500$, $T = 0$) with different isospin asymmetries, calculate their free energies with Coulomb switched off, and, from a least-squares fit, find the parameters f_v, f_s, $f_v^{\rm sym}$, and $f_s^{\rm sym}$ [cf. Eq. (27)]. We then repeat the calculations at the same temperature for several other different sets of larger masses. It is found that there is only a marginal change in f_v, f_s, and $f_v^{\rm sym}$, but $f_s^{\rm sym}$ increases with the mass of the nuclear set, tending asymptotically towards the SINM value. The same conclusion emerges again even if f_v, f_s, and $f_v^{\rm sym}$ are kept constant to the values specific for the interaction. It may be noted that from the double difference of the *experimental* symmetry energies of the finite nuclei, the value of $f_s^{\rm sym}(T = 0)$ was empirically found to be 58.91 ± 1.08 MeV [33]. As is seen from Fig. 8, the value obtained from the SK255 interaction is in consonance with this empirical value. The values from the other two interactions are somewhat lower. The latter values, however, agree closely with the value of $f_s^{\rm sym}$ obtained from the fitting of the nuclear masses [34].

IV. CONCLUSIONS

The thermal evolution of the surface properties of two-component SINM and of finite nuclei has been investigated in the present article. Calculations were performed in the FTTF framework; stability of the seemingly unstable hot nuclear systems was achieved through the subtraction procedure. Three Skyrme-class interactions, namely, SkM*, SLy4, and SK255, designed to reproduce the bulk properties of cold nuclei were employed. The dependence of the hot nuclear surface properties on the energy density functionals was thereby explored.

The combined effect of temperature and asymmetry on the nuclear surface has important bearing in astrophysics and heavy-ion collisions; in that context, for ready use, analytic expressions that fit the calculated data for SINM well over a wide range of temperatures and asymmetries are given. For hot atomic nuclei, the liquid-drop model acted as a framework for obtaining the desired thermal evolution of their surface. For applications in asymmetric systems, the need to properly match the definition of the surface energy to the volume energy has been stressed earlier [11]. Due care has been taken in this work for its implementation in both finite nuclei and in SINM; to be clear, propriety demands the evaluation of the surface thermodynamic potential, which we have done.

The dependence of the surface thermodynamic potential on temperature is seen to be of the form $[g(T, T_c(X))]^{\alpha_1}$; for SINM, α_1 has somewhat different values in different temperature ranges, rising slowly from $\sim$1.0 at low temperature to $\sim$1.26 near the critical temperature. For different interactions, α_1 is seen to have nearly the same value. For finite nuclei, the functional form of $g[T, T_c(X = 0)]$ remains the same, but α_1 is much larger, in the neighborhood of $\sim$1.45 for the three interactions that we have chosen. These are finite size effects; they leave their imprints on the surface symmetry free energy coefficient too. For finite systems, the surface symmetry energy is comparatively much smaller, rising slowly to the asymptotic value for SINM with increasing size.

ACKNOWLEDGMENTS

The authors gratefully acknowledge the assistance of Tanuja Agrawal in the preparation of the manuscript. J.N.D acknowledges support from the Department of Science & Technology, Government of India.

[1] C. F. Von Weizsäcker, Z. Phys. **96**, 431 (1935).
[2] W. D. Myers and W. J. Swiatecki, Ann. Phys. (N.Y.) **55**, 395 (1969).
[3] W. D. Myers and W. J. Swiatecki, Ann. Phys. (N.Y.) **84**, 186 (1974).
[4] D. Bandyopadhyay, C. Samanta, S. K. Samaddar, and J. N. De, Nucl. Phys. A **511**, 1 (1990).
[5] J. P. Bondorf, R. Donangelo, I. N. Mishustin, C. J. Pethick, H. Schultz, and K. Sneppen, Nucl. Phys. A **443**, 321 (1985).
[6] J. P. Bondorf, A. S. Botvina, A. S. Iljinov, I. N. Mishustin, and K. Sneppen, Phys. Rep. **257**, 133 (1995).
[7] S. Levit and P. Bonche, Nucl. Phys. A **437**, 426 (1986).
[8] D. Bandyopadhyay, J. N. De, S. K. Samaddar, and D. Sperber, Phys. Lett. B **218**, 391 (1989).
[9] A. W. Steiner, M. Prakash, J. M. Lattimer, and P. J. Ellis, Phys. Rep. **411**, 325 (2005).
[10] H.-Th. Janka, K. Langanke, A. Marek, G. Martínez-Pinedo, and B. Müller, Phys. Rep. **442**, 38 (2007).
[11] W. D. Myers, W. J. Swiatecki, and C. S. Wang, Nucl. Phys. A **436**, 185 (1985).
[12] K. Kolehmainen, M. Prakash, J. M. Lattimer, and J. Treiner, Nucl. Phys. **439**, 537 (1985).

[13] M. Centelles, M. Del Estal, and X. Viñas, Nucl. Phys. A **635**, 193 (1998).
[14] J. M. Pearson, M. Farine, and J. Conte, Phys. Rev. C **26**, 267 (1982).
[15] F. Tondeur, M. Brack, M. Farine, and J. M. Pearson, Nucl. Phys. A **420**, 297 (1984).
[16] D. G. Ravenhall, C. J. Pethick, and J. M. Lattimer, Nucl. Phys. A **407**, 571 (1983).
[17] J. N. De, S. K. Samaddar, X. Viñas, M. Centelles, I. N. Mishustin, and W. Greiner, Phys. Rev. C **86**, 024606 (2012).
[18] J. N. De, S. K. Samaddar, and B. K. Agrawal, Phys. Lett. B **716**, 361 (2012).
[19] L. D. Landau and E. M. Lifshitz, *Statistical Physics* (Pergamon, Oxford, 1980), Chap. XV.
[20] J. Bartel, P. Quentin, M. Brack, C. Guet, and H. B. Hakansson, Nucl. Phys. A **386**, 79 (1982).
[21] E. Chabanat, P. Bonche, P. Haensel, J. Meyer, and R. Schaeffer, Nucl. Phys. A **635**, 231 (1998).
[22] B. K. Agrawal, S. Shlomo, and V. Kim Au, Phys. Rev. C **68**, 031304(R) (2003).
[23] P. Bonche, S. Levit, and D. Vautherin, Nucl. Phys. A **427**, 278 (1984).
[24] P. Bonche, S. Levit, and D. Vautherin, Nucl. Phys. A **436**, 265 (1985).
[25] E. Suraud, Nucl. Phys. A **462**, 109 (1987).
[26] J. N. De, X. Viñas, S. K. Patra, and M. Centelles, Phys. Rev. C **64**, 057306 (2001).
[27] M. Brack, C. Guet, and H. B. Hakansson, Phys. Rep. **123**, 275 (1985).
[28] P. Klüpfel, P. G. Reinhard, T. J. Bürvenich, and J. A. Maruhn, Phys. Rev. C **79**, 034310 (2009).
[29] P. Papakonstantinou, J. Margueron, F. Gulminelli, and Ad. R. Raduta, Phys. Rev. C **88**, 045805 (2013).
[30] B. K. Agrawal, J. N. De, and S. K. Samaddar, Phys. Rev. Lett. **109**, 262501 (2012).
[31] M. Centelles, X. Roca-Maza, X. Viñas, and M. Warda, Phys. Rev. Lett. **102**, 122502 (2009).
[32] A. Bohr and B. Mottelson, *Nuclear Structure* (Benjamin, Reading, MA, 1969), Vol. 1.
[33] H. Jiang, G. J. Fu, Y. M. Zhao, and A. Arima, Phys. Rev. C **85**, 024301 (2012).
[34] M. Stoitsov, R. B. Cakirli, R. F. Casten, W. Nazarewicz, and W. Satula, Phys. Rev. Lett. **98**, 132502 (2007).